Geophys. J. Int. (2007) **171,** 841–846 doi: 10.1111/j.1365-246X.2007.03573.x

Influence of the Interface Fresnel zone on the reflected *P*-wave amplitude modelling

Nathalie Favretto-Cristini,[1] Paul Cristini[1] and Eric de Bazelaire[2]*

[1] *Laboratoire de Modélisation et Imagerie en Géosciences de Pau, Université de Pau, CNRS,* BP 1155, 64013 *Pau, France. E-mail: nathalie.favretto@univ-pau.fr*

[2] 11 *route du Bourg,* 64230 *Beyrie-en-Béarn, France*

Accepted 2007 July 27. Received 2007 May 13; in original form 2004 December 3

SUMMARY

The aim of the paper is to emphasize the importance of accounting for the Fresnel volume and for the Interface Fresnel zone (IFZ) for calculating the amplitude of the *P* wave emanating from a point source and recorded at a receiver after its specular reflection on a smooth homogeneous interface between elastic media. For this purpose, by considering the problem of interest as a problem of diffraction by the IFZ, that is, the physically relevant part of the interface which actually affects the reflected wavefield, we have developed a method which combines the Angular Spectrum Approach (ASA) with the IFZ concept to get the 3-D analytical solution. The variation in the reflected *P*-wave amplitude evaluated with the ASA, as a function of the incidence angle, is compared with the plane wave (PW) reflection coefficient and with the exact solution provided by the 3-D code OASES, for one solid/solid configuration and two dominant frequencies of the source. For subcritical incidence angles the geometrical spreading compensation is mostly quite sufficient to reduce the point-source amplitudes to the PW amplitudes. On the contrary, for specific regions of incidence angles for which the geometrical spreading compensation is not sufficient anymore, that is, near the critical region and in the post-critical domain, the ASA combined with the IFZ concept yields better results than the PW theory whatever the dominant frequency of the source, which suggests that the additional application of the IFZ concept is necessary to obtain the reflected *P*-wave amplitude. Nevertheless, as the ASA combined with the IFZ has been used only for evaluating the contribution of the reflected wavefield at the receiver, its predictions fail when the interference between the reflected wave and the head wave becomes predominant.

Key words: amplitude, Fresnel volume, Interface Fresnel zone, *P* wave, reflected wave, smooth interface.

INTRODUCTION

Since many decades geophysicians have developed various theoretical methods to fit the real seismic data, their ultimate goal being to invert them to retrieve the geometrical and physical characteristics of the Earth. Since the media heterogeneity can be highly complex, depending on the seismic frequency range of interest, using the exact form (in the time domain) of waves emanating from a point source and being reflected by interfaces (Aki & Richards 2002, chap. 6) can be a very difficult task for interpreting some seismic observations. Interpretation of such observations then always relies on approximations.

The basis of many seismic studies is the ray theory (Cerveny 2001). Under this approximation it is assumed that the high-frequency part of elastic energy propagates along infinitely narrow lines through space, called rays, which join the source and the receiver. Ray theory is then strictly valid only in the limit of a hypothetical infinite-frequency wave. As recorded data have a finite frequency content, it is accepted that seismic wave propagation is extended to a finite volume of space around the ray path, called the first Fresnel volume (Kravtsov & Orlov 1990), hereafter denoted FV. The wave properties are thus influenced not only by the media structure along the ray, but also by the media structure in the vicinity of the ray. This well-known limitation of ray theory has received broad attention in recent past years. The concept of FV (also known as physical ray, 3-D Fresnel zone, etc.) is continually being developed and has found so many applications in seismology and in seismic exploration, that it is impossible here to review all the books and articles which pay attention to it in seismic wave propagation. Nevertheless, we shall mention the works of Cerveny and his co-authors who have proposed two methods for including FV parameter calculations into the ray tracing procedure in complex

*Deceased on 2007, June 28th

2-D and 3-D structures. The first one, called the Fresnel volume ray tracing (Cerveny & Soares 1992), combines the paraxial ray approximation with the dynamic ray tracing and is only applicable to zero-order waves (direct, reflected and transmitted waves...), whereas the second method, more accurate than the previous one, is based on network ray tracing (Kvasnicka & Cerveny 1994). Contrary to the previous methods, the FVs can also be computed without knowledge of the velocity model of the media (Hubral *et al.* 1993). Note that analytical expressions for FVs of seismic body waves and for their intersection with interfaces, called the Interface Fresnel zones (IFZ), have been derived in Kvasnicka & Cerveny (1996a) and in Kvasnicka & Cerveny (1996b). Many works have shed new light on the role of the FVs in the seismic imaging of reflectors. They have shown that, besides being connected with the resolution of seismic methods (Sheriff 1980; Lindsey 1989; Knapp 1991), the FVs also play a role in the migration and demigration processes (Hubral *et al.* 1993; Schleicher *et al.* 1997). Moreover, FVs have been applied to inversion studies of seismic data (Yomogida 1992) and they have been incorporated into tomographic traveltime inversion schemes (Vasco & Majer 1993). Note also that in global seismology, sensitivity kernels have been developed for global tomography inversions to overcome the limitations of ray theory and to account for finite-frequency effects upon seismic wave propagation (Zhou *et al.* 2005). Sensitivity kernels (also known as Fréchet kernels) linearly relate velocity perturbations of the medium to changes in some seismic observables (traveltime, waveform, splitting intensity) of the band-limited waves (Marquering *et al.* 1999; Dahlen *et al.* 2000; Dahlen & Baig 2002; Favier & Chevrot 2003). FVs and sensitivity kernels are closely connected through the concept of constructive interferences of waves (Vasco *et al.* 1995; Spetzler & Snieder 2004).

The variability of the amplitudes of the reflected waves with the incidence angle is of great interest for many seismological applications, for instance to constrain localization of reflectors and media properties. Since the media heterogeneity can be highly complex in the typical seismic frequency range, and considering that both source and receivers are usually located far from the interfaces, the exact form of spherical waves generated by a point source is not convenient for interpreting complex seismic observations. A survey of the literature brings to light that most calculations are generally performed within the framework of monochromatic plane wave (PW) theory or finite-frequency theory without nevertheless taking into account the frequency-dependent spatial regions (i.e. FVs) in the vicinity of the ray. This is justified by the fact that for some typical configurations and for subcritical incidence angles, the geometrical spreading compensation is mostly quite sufficient to reduce the point-source amplitudes to the PW amplitudes. On the contrary, for critical and post-critical incidence angles this compensation is generally not sufficient anymore, and an additional processing should be considered. To the best of the authors' knowledge, a theoretical study of the FV and IFZ imprint on the reflected wave amplitudes for critical and post-critical angles has not been developed yet, despite the band-limited nature of seismic data. This is the purpose and scope of this work.

The paper is divided in two sections. Section 1 is mainly concerned with 3-D analytical derivations. After briefly introducing the FV and IFZ concepts, we describe the method we used for deriving the amplitude of the *P* wave emanating from a point source and recorded at a receiver after its reflection on a smooth interface between elastic media. As the problem under consideration can be viewed as a problem of diffraction by the IFZ, that is, the physically relevant part of the interface which actually affects the reflected wavefield, we applied the Angular Spectrum Approach (ASA) (Goodman 1996) to get the 3-D analytical solution. Section 2 investigates the role of the IFZ in the reflected wave propagation, more specially in the critical and post-critical regions. The variation in the reflected *P*-wave amplitude, as a function of the incidence angle, evaluated with the ASA is compared with the PW reflection coefficient, and with the exact solution obtained with the 3-D code OASES (http://acoustics.mit.edu/faculty/henrik/oases.html), for one solid/solid configuration and two dominant frequencies of the source.

1 3-D ANALYTICAL DERIVATIONS OF THE REFLECTED *P*-WAVE AMPLITUDE

1.1 Characteristics of the Interface Fresnel zone

We consider two homogeneous isotropic elastic media in welded contact at a plane interface characterized by the *xy*-plane, the vertical *z*-axis being directed downwards. The point source S($-x_S$, 0, $-z_S$) and the receiver R(x_S, 0, $-z_S$) are located at a distance z_S from the interface. The source generates in the upper medium a spherical wave with a constant amplitude. The spherical wave can be decomposed into an infinite sum of PW synchronous each other at the time origin. We consider the harmonic PW with frequency f which propagates in the upper medium with the velocity V_{P1} from S to R, after being reflected by the interface at the Cartesian coordinate origin M(0,0,0) in a specular direction θ with respect to the normal to the interface. Let the traveltime of the ray SMR be t_{SMR}.

The frequency-dependent spatial region in the vicinity of the ray SMR which actually affects the wavefield at the receiver R is known to be the FV corresponding to the source–receiver pair (S, R) and relative to the specular reflection SMR. By definition, the FV is formed by virtual points F which satisfy the following condition (Kravtsov & Orlov 1990):

$$|t(F,S)+t(F,R)-t(M,S)-t(M,R)| \leq \frac{1}{2f}, \tag{1}$$

or:

$$|l(F,S)+l(F,R)-l(M,S)-l(M,R)| \leq \frac{\lambda_1}{2}, \tag{2}$$

where $\lambda_1 = \frac{V_{P1}}{f}$ is the wavelength corresponding to the dominant frequency f of the narrow-band source signal. The quantity $t(X,Y)$ denotes the traveltime from the point X to the point Y, and $l(X,Y)$ the distance between X and Y. The boundary of the FV is then given by the following equation:

$$|l(F,S)+l(F,R)-l(M,S)-l(M,R)| = \frac{\lambda_1}{2}. \tag{3}$$

Here, it must be specified that, as seismic wavefields are transient and large-band, it is generally necessary to decompose the source signal into narrow-band signals for which monochromatic FV can be constructed for the prevailing frequency of the signal spectrum (Knapp 1991). The physical meaning of eq. (2), describing the FV concept, is quite obvious: the waves passing through the diffraction points F interfere constructively with the specular reflected wave when the path-length difference is less than one-half of the wavelength λ_1. As is well known, the main contribution to the wavefield comes from the first FV as the rapid oscillatory responses of the higher-order FVs and Fresnel zones cancel out and give minor contributions to the wavefield (Born & Wolf 1999). That is why in our work we restrict ourselves to the first FV which will be simply referred to as FV.

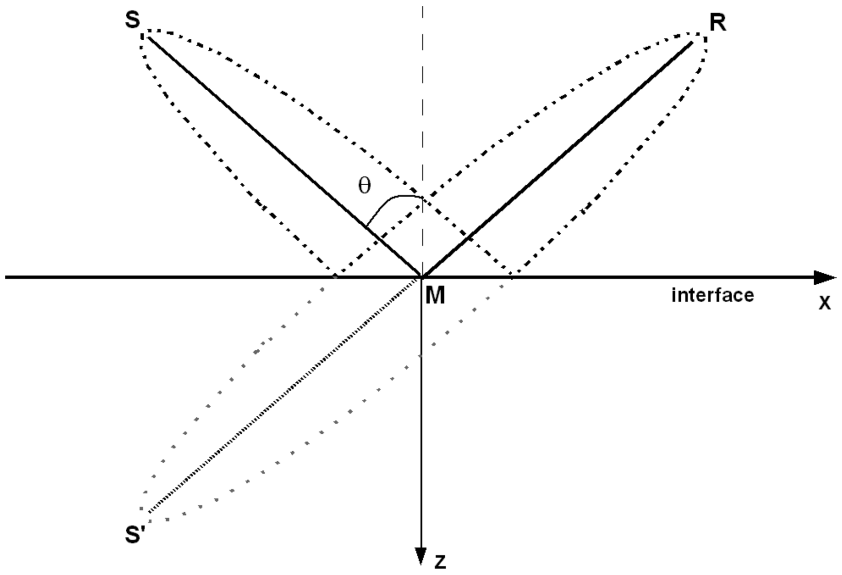

Figure 1. Representation in the *xz*-plane of the Fresnel volume involved in the wave reflection at the point M at a plane homogeneous interface, under the incidence angle θ. The source S and the receiver R are located at a distance z_S from the interface. The classical representation of the Fresnel volume is the ellipsoid of revolution with foci located at R and at the image source S' situated symmetrically to the point source S on the other side of interface. The Interface Fresnel zone is characterized by the intersection of the ellipsoid of revolution (Fresnel volume) with the interface plane.

The IFZ is defined as the cross-section of the FV by an interface which may not be perpendicular to the ray SMR. If the source S and the receiver R are situated at the same distance from the interface, the IFZ is represented by an ellipse centred at the reflection point M. The common way of determining the size of the IFZ is to consider the FV represented by the ellipsoid of revolution with foci at the receiver R and at the image source S' situated symmetrically to S on the other side of interface (Fig. 1). The boundary of this FV is then given by the following equation:

$$|l(F, S') + l(F, R) - l(M, S') - l(M, R)| = \frac{\lambda_1}{2}, \tag{4}$$

or in the Cartesian coordinates (x, y, z) after some straightforward calculations:

$$\frac{(x\ \sin\theta - z\ \cos\theta)^2}{\left(\frac{z_S}{\cos\theta} + \frac{\lambda_1}{4}\right)^2} + \frac{y^2 + (x\ \cos\theta + z\ \sin\theta)^2}{\frac{\lambda_1}{2}\left(\frac{z_S}{\cos\theta} + \frac{\lambda_1}{8}\right)} = 1. \tag{5}$$

The boundary of the IFZ is then obtained from the formulation of the ellipsoid of revolution, eq. (5), equating the variable z to zero:

$$\frac{x^2}{r^{\parallel 2}} + \frac{y^2}{r^{\perp 2}} = 1, \tag{6}$$

where the in-plane semi-axis $r^{\parallel}$, corresponding to the plane of incidence, and the transverse semi-axis $r^{\perp}$, corresponding to the direction perpendicular to the plane of incidence, of the IFZ are expressed as (Kvasnicka & Cerveny 1996a):

$$r^{\parallel} = \left[\frac{\lambda_1}{2}\left(\frac{z_S}{\cos\theta} + \frac{\lambda_1}{8}\right)\right]^{\frac{1}{2}}\left[1 - \frac{z_S^2\tan^2\theta}{\left(\frac{z_S}{\cos\theta} + \frac{\lambda_1}{4}\right)^2}\right]^{-\frac{1}{2}},$$

$$r^{\perp} = \left[\frac{\lambda_1}{2}\left(\frac{z_S}{\cos\theta} + \frac{\lambda_1}{8}\right)\right]^{\frac{1}{2}}. \tag{7}$$

The characteristics of the IFZ depend on the position of the source–receiver pair, and also on the incidence angle of the ray SM. Moreover, larger portions of the interface (reflector) are involved for low-frequency than for high-frequency components of the wavefield. It is also well known that a perturbation of the medium actually affects the reflected wave when this perturbation is located inside the IFZ.

1.2 Analytical expression for the reflected *P*-wave amplitude

We consider the same previous configuration. Let the orthotropic source be located at the point S, far from the plane interface between two homogeneous isotropic elastic media. The spherical *P* wave emanating from the source propagates obliquely in the upper medium and strikes the interface. It is then reflected from the interface and finally recorded at the receiver located at the point *R*, far from the interface. Our objective is to calculate the amplitude of the reflected wavefield measured at the receiver, by accounting for the FV and the IFZ which physically contribute to the wave propagation process.

The problem under consideration can be viewed as a problem of diffraction by the physically relevant part of the interface (namely, the IFZ). We chose to apply the ASA (Goodman 1996) to get the 3-D analytical solution to this problem. The motivations of this choice are twofold. Provided the spherical wavefield is decomposed by Fourier analysis into a linear combination of elementary plane wavesurfaces, travelling in different directions away from the source, the effect of propagation over distance is simply a change of the relative phases of the various plane wavesurface components. Moreover, despite their apparent differences, the ASA and the first Rayleigh-Sommerfeld solution (Goodman 1996, chap. 3, p. 47) yield identical predictions of diffracted fields (Sherman 1967). The advantage of using the ASA then seems obvious: it permits straightforward derivations of the measured amplitude of the reflected wave at the point R. We refer to the book of Goodman (Goodman 1996, chap. 3, pp. 55–61) for a detailed treatment of the ASA.

When using the ASA, we have to remind that it is a technique for modelling the propagation of acoustic fields between parallel planes. Considering the case of the field reflection from an oblique interface then requires several steps including rotational transformation of

complex amplitudes in the Fourier domain. This step which is the most essential and significant operation in the problem of interest here causes various problems. The non-linearity of the rotational transformation has to be taken into account and a Jacobian must be introduced. The rotational transformation also causes numerical problems, more specifically the distortion of equidistant sampling grid of the field and a shift in the centre frequency in the resulting spectrum, which makes the standard Fast Fourier Transform (FFT) algorithm inapplicable. Efficient solutions to these problems can be found in (Matsushima *et al.* 2003). We refer to the paper of Matsushima and his collaborators for a detailed treatment of these solutions.

The procedure of the method we used to get the amplitude of the reflected wavefield measured at the receiver can be summarized as follows. At the interface $z = 0$, and more precisely within the IFZ, the amplitude U generated by the point source S and diffracted by the IFZ has a 2-D Fourier transform given by:

$$A\left(f_x, f_y, 0, \theta\right) = \int\int_{-\infty}^{+\infty} U\left(x, y, 0, \theta\right) \exp\left[-j2\pi\left(f_x x + f_y y\right)\right] \mathrm{d}x\mathrm{d}y \qquad (8)$$

where $U\left(x, y, 0, \theta\right) = \frac{e^{j\frac{2\pi f}{V_{P1}} R_M}}{R_M} H\left(x, y, \theta\right)$ with $R_M = \sqrt{x^2 + y^2 + z_I^2}$ and $z_I = z_S/\cos\theta$.

The function $H\left(x, y, \theta\right)$ represents the size of the IFZ which is a function of the incidence angle θ:

$$\begin{cases} H\left(x, y, \theta\right) = 1 & \text{if } (x, y) \in IFZ \\ H\left(x, y, \theta\right) = 0 & \text{if } (x, y) \notin IFZ \end{cases}$$

The term $A\left(f_x, f_y, 0, \theta\right)$ represents the plane wave decomposition of the incident wavefield, that is, the angular spectrum. The direction cosines of each plane wave associated with the frequencies (f_x, f_y) are given by (Goodman 1996):

$$\alpha = \lambda_1 f_x\,, \quad \beta = \lambda_1 f_y, \quad \gamma = \sqrt{1 - \alpha^2 - \beta^2}.$$

As the incident wavefield is reflected from the interface, the angular spectrum of the resulting wavefield is obtained by multiplying $A\left(f_x, f_y, 0, \theta\right)$ by the classical plane wave reflection coefficient $R\left(f_x, f_y, \theta\right)$ given by Zoeppritz equations (Aki & Richards 2002):

$$A_R(f_x, f_y, 0, \theta) = A(f_x, f_y, 0, \theta)\, R(f_x, f_y, \theta). \qquad (9)$$

The reflection coefficient takes into account the fact that the central ray is incident on the interface under the incidence angle θ. The angular spectrum $A_R(\tilde{f}_x, \tilde{f}_y, 0, \theta)$ is then calculated from $A_R(f_x, f_y, 0, \theta)$ for the interface plane rotated by θ clockwise about the origin M. This plane is perpendicular to the specularly reflected ray passing through the point M. At this step, we must multiply the angular spectrum $A_R(\tilde{f}_x, \tilde{f}_y, 0, \theta)$ by the Jacobian $J(\tilde{f}_x, \tilde{f}_y, \theta)$ resulting from the rotational transformation in order to get the correct energy of each plane wave component. The resulting angular spectrum in the rotated plane is:

$$\tilde{A}_R(\tilde{f}_x, \tilde{f}_y, 0, \theta) = A_R(\tilde{f}_x, \tilde{f}_y, 0, \theta)\, |J(\tilde{f}_x, \tilde{f}_y, \theta)|. \qquad (10)$$

We must also apply a method of interpolation to obtain an equidistant sampling grid of the spectrum, as suggested in (Matsushima *et al.* 2003). The angular spectrum $\tilde{A}_R(\tilde{f}_x, \tilde{f}_y, 0, \theta)$ is then propagated to the parallel plane passing through the receiver R. The resulting spectrum is expressed as:

$$\tilde{A}_R(\tilde{f}_x, \tilde{f}_y, -z_S, \theta) = \tilde{A}_R(\tilde{f}_x, \tilde{f}_y, 0, \theta)\, \exp\left[j\, 2\pi\gamma\, \frac{z_I}{\lambda_1}\right]. \qquad (11)$$

Table 1. Properties of the homogeneous, isotropic, and elastic media in contact. ρ, V_P and V_S denote, respectively, the density, *P*- and *S*-wave velocities for the upper (subscript 1 in the text) and lower media.

Properties	V_P (m s^{-1})	V_S (m s^{-1})	ρ (kg m^{-3})
Upper medium	4000	2000	2000
Lower medium	5200	2500	2400

By using inverse Fourier transform, we get the amplitude of the reflected wavefield:

$$U_R(\tilde{x}, \tilde{y}, -z_S, \theta) = \int\int_{-\infty}^{+\infty} \tilde{A}_R(\tilde{f}_x, \tilde{f}_y, -z_S, \theta)\, \exp[j2\pi(\tilde{f}_x\tilde{x} + \tilde{f}_y\tilde{y})]\mathrm{d}\tilde{x}\, \mathrm{d}\tilde{y}. \qquad (12)$$

Since the receiver is located at the centre of the plane, the amplitude of the reflected wavefield at the receiver is finally given by $U_R\,(0, 0, -z_S, \theta)$.

2 COMPARISON WITH THE EXACT SOLUTION AND WITH THE PLANE WAVE THEORY PREDICTION

The aim of this section is to evaluate the importance of using the band-limited data concept, based on the IFZ, in order to simulate the amplitudes of the reflected waves recorded at receivers. For this purpose, it is instructive to compare the variation in the amplitude obtained with our approximation (ASA combined with the IFZ concept), as a function of the incidence angle, with the amplitude predicted by a numerical code which provides the exact solution, and with the amplitude predicted by the classical PW theory [here, the Zoeppritz equations (Aki & Richards 2002)]. We used the 3-D code OASES (http://acoustics.mit.edu/faculty/henrik/oases.html) to compute accurately synthetic seismograms in media. OASES is a general purpose computer code for modelling seismo-acoustic propagation in horizontally stratified media using wavenumber integration in combination with the Direct Global Matrix solution technique (Schmidt & Jensen 1985; Schmidt & Tango 1986; Jensen *et al.* 1994). In seismology, the wavenumber integration methods are often referred to as reflectivity methods or discrete wavenumber methods (Fuchs & Muller 1971; Bouchon 1981; Kennett 1983; Olson *et al.* 1984; Muller 1985). This software has the great advantage of providing reference solutions for various types of sources (explosive source, vertical point force, etc.). In addition, upward and downward propagation of compressional and of shear waves can be easily separated. This 3-D code is widely used in the underwater acoustics community and has been thoroughly validated.

One case of interface between elastic media whose properties are reported in Table 1 has been chosen to illustrate the theoretical results. The interface is situated at a distance $z_S = 3000$ m from the source–receiver plane. For the 3-D code the amplitude of the source signal is chosen to be the Fourier transform of a Ricker wavelet with either the dominant frequency $f = 32$ Hz and the frequency bandwidth $B = 10$ Hz, or $f = 12$ Hz and $B = 6$ Hz.

Fig. 2 depicts the amplitude-versus-angle (AVA) curves provided by the exact solution and by our approximation for the frequencies $f = 32$ and 12 Hz, and the AVA curves provided by the PW theory which does not depend on frequency. A geometrical spreading compensation factor equal to $\frac{z_S}{\cos\theta}$ was applied to the predictions of our 3-D approximation and to the synthetic data provided by the 3-D code OASES, in order to be compared in a suitable way with the

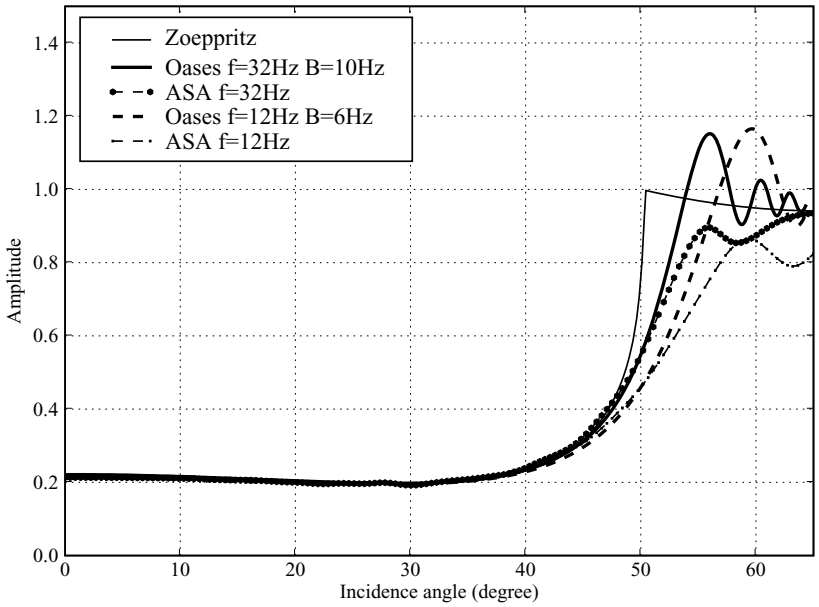

Figure 2. Variation of the amplitude of the P wave reflected from a plane interface, as a function of the incidence angle. Comparison between the plane wave reflection coefficient and the spreading-free amplitudes associated with the exact solutions and with the approximate solutions. The exact solutions were provided by the 3-D code OASES. The source signal was a Ricker wavelet with either the dominant frequency $f = 32$ Hz and the frequency bandwidth $B = 10$ Hz, or $f = 12$ Hz and $B = 6$ Hz. The approximate solutions were obtained by applying the Angular Spectrum Approach together with the Interface Fresnel Zone concept for $f = 32$ and 12 Hz.

PW predictions. Inspection of Fig. 2 shows that for small subcritical angles, AVA curves associated with the exact (OASES) solution and AVA curves associated with the PW theory are quite identical. The discrepancies between them do not exceed 1.4 per cent (for $f = 12$ Hz) and 1 per cent (for $f = 32$ Hz) up to $\theta = 40^\circ$. As the PW reflection coefficient varies smoothly with the incidence angle, the geometrical spreading compensation is sufficient to reduce the amplitude of the reflected wave generated by the point source to the reflected PW amplitude. The effect of the IFZ on the wave amplitude, is therefore, negligible for small incidence angles in the subcritical region. Between $\theta = 40^\circ$ and the critical angle $\theta_C = 50.28^\circ$, the PW reflection coefficient rapidly increases with the incidence angle, and the geometrical spreading compensation is not sufficient anymore. The discrepancies between the exact curves and the PW reflection coefficient increase monotonically with the incidence angle and exceed 105 per cent (for $f = 12$ Hz) and 70 per cent (for $f = 32$ Hz) for θ_C. Therefore, the additional application of the IFZ concept becomes necessary to get the reflected P-wave amplitude. Note that the discrepancies between the exact solution and the reflection coefficient also increase with decreasing frequencies. The PW theory does not yield reasonable results for low frequencies.

In Fig. 2 we can also note that near the critical angle, the predictions of our approximation which combines the ASA and the IFZ concept yields better results than the PW reflection coefficient, more particularly between $\theta = 40^\circ$ and θ_C. Whatever the frequency, the discrepancies between the ASA curves and the exact curves do not exceed 5 per cent up to $\theta = 52^\circ$ and are smaller than 1 per cent for $\theta_C = 50.28^\circ$. Nevertheless, with increasing incidence angle, the approximate solutions show increasing discrepancies in comparison with the corresponding exact solutions. The discrepancies reach the maximum value of 26 per cent for $\theta = 60^\circ$ and $f = 12$ Hz, and the maximum value of 22 per cent for $\theta = 56^\circ$ and $f = 32$ Hz. Beyond these angles they sharply decrease with increasing incidence angles.

The explanation of the discrepancies between our approximate solutions and the exact ones may come from the fact that we calculated only the reflected wave amplitude, whereas the code OASES provides the amplitude of the interference between the reflected and the head wavefields. The contribution of each wavefield to the global amplitude at the receiver cannot be discriminated in the synthetic seismograms because both waves have the same traveltime for a specific range of incidence angles. In fact, it would be interesting to get the amplitude of the head wave by using the combination of the ASA with the IFZ concept associated with this particular wave, in order to determine the contribution of the reflected wave and the contribution of the head wave at the receiver, taking into account the phase shifts. This would enlighten on the complex physical process of wave interference with the reflected wave. Our present work is focused precisely on this particular aspect and will be reported later.

CONCLUSION

The aim of the paper was to discuss the influence of the IFZ for modelling the amplitude of the P wave emanating from a point source and recorded at a receiver after its specular reflection on a smooth interface between two elastic media. As the problem of interest can be viewed as a problem of diffraction by the IFZ, that is, the physically relevant part of the interface which actually affects the reflected wavefield, we have applied the ASA combined with the IFZ concept to get the 3-D analytical solution. The variation in the reflected P-wave amplitude obtained with the ASA, as a function of the incidence angle, has been compared for one solid/solid configuration and two frequencies of the source with the PW reflection coefficient and with the exact solution obtained with the 3-D code OASES. It results that for subcritical incidence angles the geometrical spreading compensation is mostly quite sufficient to reduce the point-source amplitudes to the PW amplitudes. On the contrary, near the critical region, the ASA combined with the IFZ

concept yields better results than the PW theory whatever the dominant frequency of the source. These results suggest that near and beyond the critical region the geometrical spreading compensation is not sufficient anymore, and that the additional application of the IFZ concept, therefore, becomes necessary to obtain the reflected *P*-wave amplitude. As in the paper our approximation is concerned only with the reflected wavefield, its predictions fail in the post-critical region when the interference between the reflected wave and the head wave becomes predominant. For a further validation of our method, we need to evaluate the contribution of the head wave at the receiver by taking into account its own IFZ, in order to combine it with the contribution of the reflected wavefield at the receiver. Our present work is focused precisely on this particular aspect and will be reported later.

ACKNOWLEDGMENTS

The manuscript has been significantly improved thanks to the relevant suggestions of anonymous reviewers and the editor. We appreciate the time and effort that they invested in our study and we gratefully acknowledge them.

The work reported here is the result of fruitful collaboration with our friend Dr Eric De Bazelaire during many years. We consider ourselves extremely fortunate to have had the opportunity to work at close quarters with a scientist of his calibre, and more specially to have stroken up a profound friendship with him.

REFERENCES

Aki, K. & Richards, P., 2002. *Quantitative Seismology*, 2nd edn, University Science Books, Sausalito, CA, USA.

Born, M. & Wolf, E., 1999. *Principles of Optics*, 7th expanded edn, Cambridge University Press, Cambridge, UK.

Bouchon, M., 1981. A simple method to calculate Green's functions for elastic layered media, *Bull. seism. Soc. Am.,* **71,** 959–971.

Cerveny, V., 2001. *Seismic Ray Theory*, Cambridge University Press, Cambridge, UK.

Cerveny, V. & Soares, J.E.P., 1992. Fresnel volume ray-tracing, *Geophysics,* **57,**(7), 902–915.

Dahlen, F.A. & Baig, A.M., 2002. Fréchet kernels for body wave amplitudes, *Geophys. J. Int.,* **150,** 440–466.

Dahlen, F.A., Hung, S.-H. & Nolet, G., 2000. Fréchet kernels for finite-frequency traveltimes-I. Theory, *Geophys. J. Int.,* **141,** 157–174.

Favier, N. & Chevrot, S., 2003. Sensitivity kernels for shear wave splitting in transverse isotropic media, *Geophys. J. Int.,* **153,** 213–228.

Fuchs, K. & Muller, G., 1971. Computation of synthetic seismograms with the reflectivity method and comparison of observations, *Geophys. J. R. astr. Soc.,* **23,** 417–433.

Goodman, J.W., 1996. *Introduction to Fourier Optics*, 2nd edn, MacGraw-Hill, New York, USA.

Hubral, P., Schleicher, J., Tygel, M. & Hanitzch, C., 1993. Determination of Fresnel zones from traveltime measurements, *Geophysics,* **58**(5), 703–712.

Jensen, F.B., Porter, M.B., Kuperman, W.A. & Schmidt, H., 1994. *Computational Ocean Acoustics*, American Institute of Physics, New York.

Kennett, B.L.N., 1983. *Seismic Wave Propagation in Stratified Media*, Cambridge University Press, Cambridge.

Knapp, R.W., 1991. Fresnel zones in the light of broadband data, *Geophysics,* **56**(3), 354–359.

Kravtsov, Yu.A. & Orlov, Yu.I., 1990. *Geometrical Optics of Inhomogeneous Media*, Springer Series on Wave Phenomena, Springer-Verlag, NY.

Kvasnicka, M. & Cerveny, V., 1994. Fresnel volumes and Fresnel zones in complex laterally varying structures, *J. Seism. Explor.,* **3,** 215–230.

Kvasnicka, M. & Cerveny, V., 1996a. Analytical expressions for Fresnel volumes and interface Fresnel zones of seismic body waves. Part 1: direct and unconverted reflected waves, *Stud. Geophys. Geod.,* **40,** 136–155.

Kvasnicka, M. & Cerveny, V., 1996b. Analytical expressions for Fresnel volumes and interface Fresnel zones of seismic body waves. Part 2: transmitted and converted waves. Head waves, *Stud. Geophys. Geod.,* **40,** 381–397.

Lindsey, J., 1989. The Fresnel zone and its interpretative significance, *The Leading Edge,* **8,**(10), 33–39.

Marquering, H., Dahlen, F.A. & Nolet, G., 1999. Three-dimensional sensitivity kernels for finite-frequency traveltimes: the banana-doughnut paradox, *Geophys. J. Int.,* **137,** 805–815.

Matsushima, K., Schimmel, H. & Wyrowski, F., 2003. Fast calculation method for optical diffraction on tilted planes by use of the angular spectrum of plane waves, *J. Opt. Soc. Am. A,* **20,**(9), 1755–1762.

Muller, G., 1985. The reflectivity method: a tutorial, *J. Geophys.,* **58,** 153–174.

Olson, A.H., Orcutt, J.A. & Fisher, G.A., 1984. The discrete wavenumber/finite element method for synthetic seismograms, *Geophys. J. R. astr. Soc.,* **77,** 412–460.

Schleicher, J., Hubral, P., Tygel, M. & Jaya, M.S., 1997. Minimum apertures and Fresnel zones in migration and demigration, *Geophysics,* **62,** 183–194.

Schmidt, H. & Jensen, F.B., 1985. A full wave solution for propagation in multilayered viscoelastic media with application to Gaussian beam reflection at fluid-solid interfaces, *J. Acoust. Soc. Am.,* **77,** 813–825.

Schmidt, H. & Tango, G., 1986. Efficient global matrix approach to the computation of synthetic seismograms, *Geophys. J. R. astr. Soc.,* **84,** 331–359.

Sheriff, R.E., 1980. Nomogram for Fresnel-zone calculation, *Geophysics,* **45,**(5), 968–972.

Sherman, G.C., 1967. Application of the convolution theorem to Rayleigh's integral formulas, *J. Opt. Soc. Am.,* **57,** 546–547.

Spetzler, J. & Snieder, R., 2004. The Fresnel volume and transmitted waves: a tutorial, *Geophys. J. Int.,* **69,**(3), 653–663.

Vasco, D.W. & Majer, E.L., 1993. Wavepath traveltime tomography, *Geophys. J. Int.,* **115,** 1055–1069.

Vasco, D.W., Peterson, J.E. Jr & Majer, E.L., 1995. Beyond ray tomography: wavepaths and Fresnel volumes, *Geophysics,* **60,**(6), 1790–1804.

Yomogida, K., 1992. Fresnel zone inversion for lateral heterogeneities in the earth, *Pure Appl. Geophys.,* **138,**(3), 391–406.

Zhou, Y., Dahlen, F.A., Nolet, G. & Laske, G., 2005. Finite-frequency effects in global surface-wave tomography, *Geophys. J. Int.,* **163,** 1087–1111.